SPACE CAPACITY METHODOLOGIES TO RANK THE RISK OF ORBITAL REGIONS

Andrea Muciaccia(1), Camilla Colombo(1), Darren McKnight(2), Erin Dale(2), Alessandro Rossi(3)

(1) Department of Aerospace Science and Technology, Politecnico di Milano, Via Giuseppe La Masa 34, 20156, Milan, Italy, Email: andrea.muciaccia@polimi.it, camilla.colombo@polimi.it
(2) LeoLabs, 4795 Meadow Wood Lane, Chantilly, VA 20120, USA, Email: darren@leolabs.space, edale@leolabs.space
(3) IFAC-CNR, Via Madonna del Piano 10, 50019, Sesto Fiorentino, Italy, Email: a.rossi@ifac.cnr.it

ABSTRACT

The growth in the number of objects in Earth orbit poses a threat to space safety and space sustainability. The orbital space is not infinite, but it is a limited resource that must be properly managed and maintained.

In this work, three approaches to assess the *space consumed capacity* are compared on the same object population with clear distinctions between operational and non-operational objects; the three methods are THEMIS space debris indicator (Tracking the Health of the Environment and Missions In Space), the Criticality of Spacecraft Index (CSI), and the Risk Balance Model. The evaluation is performed on specific altitude bins in the Low Earth Orbit (LEO), considering different bin sizes to investigate how this affects the evaluation of the capacity at different altitude shells. The numerical results are normalised to better compare the different approaches and the relative importance of the altitude bins, ranking them from highest to lowest.

1 INTRODUCTION

The continued growth in space activities, from large-scale satellite constellations to an increasing number of small satellite launches [1], and the many fragmentations over the years, which have increased the number of uncontrollable objects in orbit [1,2], has led to intensified concern over the sustainability of the orbital environment. With more actors operating in space, the near-Earth environment faces increasing congestion and collision risks, raising questions about how much activity the orbits around the Earth can safely accommodate.

In response to these concerns, in the past years environmental impact indices [3,4] and orbital capacity models have been defined and investigated for assessing how many satellites, debris objects, or missions a given orbital region can sustainably support. These models typically account for variables such as object mass, orbital lifetime, collision risk, debris mitigation strategies, and satellite design and disposal practices. However, each model has its own assumptions, data inputs, and methodologies, making it challenging to compare their outputs [4] or adopt them as a basis for unified operational decisions.

Initially, studies focused on developing metrics to define the impact of objects on the space environment, leading to the creation of various mission-based models [5,6,7,8,9,10], which focus on the impact of a single object, and environment-based models [11,12,13,14], which assess the overall debris environment; the comparison of these models is essential for achieving a better understanding and a shared definition of this issue.

More recently, the space debris community has begun discussing the issue of space carrying capacity and how it should be measured to maintain a balance in the space environment and future launches. The models proposed so far attempt to evaluate the maximum number of objects that can be safely maintained in orbit [15], or they utilise the mission-based metrics in an aggregated manner to find a relationship between the mission's environmental impact and the level of consumed capacity [4].

In view of these considerations, this work follows previous research [3] and aims to compare three space capacity models by identifying the most important parameters and common aspects, thereby contributing to a better understanding of these models. The three methods are THEMIS space debris indicator (Tracking the Health of the Environment and Missions In Space) [9], the Criticality of Spacecraft Index (CSI) [6], and the Risk Balance Model [3]. The evaluation is performed on

Proc. 9th European Conference on Space Debris, Bonn, Germany, 1–4 April 2025, published by the ESA Space Debris Office
Editors: S. Lemmens, T. Flohrer & F. Schmitz, (http://conference.sdo.esoc.esa.int, April 2025)

specific altitude bins in the Low Earth Orbit (LEO).

Indeed, the ultimate objective of all the space capacity models is to provide support for future decisions regarding space development, offering scientific support for the identification and improvement of space policies, space traffic management decisions, and the definition of remediation strategies.

The other sections of the paper are organised as follows. Section 2 introduces the three models used, showing the main ingredients considered. Section 3 describes the reference scenario considered for the analysis and the parameters considered for comparison, while Section 4 displays the results obtained, showing similarities and differences across the three models. Finally, Section 5 concludes the article by summarising the main achievements and introducing future work.

2 SPACE CAPACITY EVALUATION MODELS

This section is devoted to a description of the three space capacity models compared in this work, namely THEMIS, Risk Balance Model, and CSI.

2.1 THEMIS

In the THEMIS model, the space capacity consumed by a defined population of orbiting objects is computed by aggregating the results of the debris index of each mission as [16]

$$\mathrm{C} = \sum I_{t_j} \tag{1}$$

where $I_{t,j}$ is the index of the *j-th* object considered in the set. In this view, the index can be currently seen as the share of the capacity of the specific mission under analysis.

The evaluation of $I_{t,j}$ is carried out using a metric defined as a risk indicator, following the original formulation of the Environmental Consequences of Orbital Breakups (ECOB)[4] index and further extended to work in orbital regions outside the LEO [17] and with different mission architectures (e.g., single satellite, constellation, etc.) [18]. The evaluation is based on selecting and analysing specific Keplerian orbital elements customised to each orbital region, focusing on those most critical for mission design and debris evolution. Focusing on the LEO orbital region, the evaluation is performed considering the semi-major axis and inclination. The evaluation is performed at different epochs and phases of the mission to observe the impact of each; in this way, the total impact of the mission I_t can be established as

$$I_t = \int_{t_0}^{t_{EOL}} I\,dt + \alpha \cdot \int_{t_{EOL}}^{t_{end}} I\,dt + (1-\alpha) \cdot \int_{t_{EOL}}^{t_f} I\,dt \tag{2}$$

where the first term of the Eq. 2 refers to the operational phase of the object, while the second and the third term refer to the Post Mission Disposal (PMD) phase where it is contemplated that the End-Of-Life (EOL) disposal may fail. The latter is taken into account through the PMD reliability α, ranging between 0 (fail) and 1 (fully reliable). Instead, I refers to the evaluation of the index at a single epoch, and is defined as follows [7]

$$I = \mathrm{p_c} \cdot e_c + p_e \cdot e_e \tag{3}$$

with p_c and p_e the probability of collision and explosion, and e_c and e_e the severity of collision and explosion (i.e., the effects of the breakup in given orbital region), respectively.

Although not directly explicit, the formulation internally considers many factors such as

- The mass and the cross-sectional area of the s/c
- The evolution of the Keplerian orbital parameters along the mission
- The collision avoidance maneuver capabilities (and their efficacy)
- The type of PMD (e.g. reentry or graveyard orbits)

2.2 Risk Balance Model

The risk balance model considers orbital capacity as a function of an ensemble of objects' risk burden posed (RBP) and risk abatement (RBA) for a given altitude.

This model is represented mathematically as

$$OC = \sum [RBP \cdot (10 - RBA) \cdot AA] \quad (4)$$

where RBP (intact object) is the product of the mass of each object multiplied by its area, and AA is the altitude adjustment (objects persists at higher altitudes).

Assuming an area-to-mass ratio, A/M = 0.01 m^2/kg for intact objects, A = 0.01M as default. Newer, constellation members typically have a larger A/M ratio; some as high as 0.05 m^2/kg.

$$RBP\ (intact\ object) = 0.01M^2 \quad (5)$$

RBP (catalogued fragments and lethal non-trackable (LNT)) are not covered in current model since collisions by them create relatively fewer objects compared to two intact objects.

- RBA (intact derelict) = 0, means no risk is abated
- RBA (operational payload, OPL) = f(manoeuvrability, PC to manoeuvre, and PC abatement goal) = 2.15 x {MAN x 0.33}x2.15 x {1 – ([6 +$\log_{10}${RMM/PC}]^2/10)}x2.15 x {1 – ([7 +$\log_{10}${AbPC}]^2/10)}

The constant 2.15 is the cube root of ten; this is used to give each factor equal weight. The manoeuvrability (MAN) taxonomy, is scored between zero and three, based on ΔV total and responsiveness of propulsion system. A default of two was used in this paper for a majority of operational payloads when discrete responsiveness was unknown.

RRM/PC threshold is the probability of collision (PC) on which a risk reduction manoeuvre (RRM) is executed, with a minimum of 10^{-6} and a default for uncrewed systems of $5 \cdot 10^{-4}$. AbPC is the goal to which the conjunction PC is to be abated, with a minimum of 10^{-7} and a default value of 10^{-5}.

AA = 1 + [(ALT-300)/100]$^{3.85}$, adjusts for persistence at altitudes >300 km from atmospheric drag.

The orbital lifetimes in this paper are derived from the analytic approach taken by Desmond King-Hele [26]. This approach permits simple excursions based on different altitudes, solar activity, and area-to-mass ratios. We do correct for the known variable coefficient of drag in LEO (2.1 near re-entry, up to 3.0 above 1,000 km altitude) while King-Hele used a value of 2.1 throughout the orbital decay process. A typical intact object has roughly a 5-year orbital lifetime at 500 km and a 25-year orbital lifetime at 615 km, based on average solar activity. Solar radiation pressure is ignored by King-Hele and thus neglected in our preliminary analysis. The exponent 3.85 was chosen to most closely match the atmospheric density as a function of altitude in LEO as derived from King-Hele.

Energetic sources onboard are ignored but could be added for future model developments.

Catalogued fragments and LNT debris are considered in this evaluation. However, if included, RBP (fragment) = 0.025 kg, by assuming A/M (fragment) = 0.05 m^2/kg and mass(fragment) = 0.5 kg and RBP (LNT) = $2.5 \cdot 10^{-6}$ kg assuming A/M (LNT) = 0.10 m^2/kg and mass (LNT) = 0.005 kg. RBA (fragment or LNT) = 0.

2.3 Criticality of Spacecraft Index

The Criticality of Spacecraft Index (CSI), *Ξ*, is a dimensionless quantity originally devised to quantify the risk posed by an abandoned object in LEO. Its formulation is fully described in [6], hence only the main features are recalled here. Given an object with mass *M* abandoned in space, we define:

$$\Xi = \frac{M}{M_0}\frac{A}{A_0}\frac{\rho}{\rho_0}\frac{L}{L_0} f(i) \quad (6)$$

where:

- *M* is the mass of the object (obtained by any reliable source, such as, e.g., the ESA DISCOS database);
- *A* is the cross-sectional area of the object (obtained by the same source as for the mass);
- *ρ* is the spatial density associated with the orbital shell where the object is residing each year computed by evolving over several decades a reference scenario of the space debris environment (obtained by the MASTER population) with SDM 4.2 [21];
- *L* is the lifetime of the object at the altitude corresponding to the shell where the object is orbiting, computed through a fit to the lifetime profile of standard objects in LEO;
- *f(i)* is a function of the orbital inclination *i*,

reflecting the fact that the collision risk is maximum for high inclination orbits.

The terms M_0, A_0, ρ_0, and L_0 are normalising factors for the mass, the area, the spatial density and the lifetime, respectively. The index Ξ was expressly devised with a simple analytical formulation to allow its reproducibility and is particularly suited to provide a quick indication of the danger to the environment posed by an object with no more manoeuvring capability abandoned in a crowded region of space.

In the most recent formulation of the CSI an additional term was included in the computation of Eq. (1). For each object in the considered population, the Minimum Orbital Intersection Distance (MOID) was computed against all the other objects. The MOID gives the absolute minimum of the distance between the points lying on two Keplerian ellipses. Its computation allows to evaluate the risk of collision between two objects in crossing Keplerian orbits. We computed the critical points of the squared distance between the orbits of each object was computed by means of the algorithm described in [22,23]. As mentioned above, this gives an estimation of the collision risk faced by an object with respect to the rest of the population, given the orbital characteristics of the considered ensemble (e.g., [24]). Then the median of the MOID ($med(MOID)_i$) is computed for all the objects. Finally, the index computed for each object using Eq. (1) is multiplied by a normalized MOID term which is

$$CR = \frac{\min\left(\mathrm{med}(\mathrm{MOID})\right)}{\mathrm{med}(\mathrm{MOID})_\mathrm{i}} \tag{7}$$

where the term at the nominator is the minimum median MOID of all the objects in the population (hence, the normalization limits the MOID term between 0 and 1).

Hence, the final formulation for the CSI used in this work is given by:

$$\Xi_{\mathrm{MOID}} = CR\,\frac{M}{M_0}\frac{A}{A_0}\frac{\rho}{\rho_0}\frac{L}{L_0}\,f(i) \tag{8}$$

Building on this original formulation, the shell criticality was developed in [19]. This is based on the concept of fractional criticality. Dividing the LEO environment in M spherical shells of altitude thickness D, we can compute, using Kepler's equation, the fractional contribution of the altitude shell j to the criticality index of any object k in an eccentric orbit as:

$$\Xi_{k,j} = \phi_{k,j}\,CR_k\,M_k A_k \rho_k L_k\,f(i) \tag{9}$$

where $\Phi_{k,j}$ is the fraction of orbital period that the object k spends inside the shell j. Thus, the overall criticality of an altitude shell can be computed because of the individual criticalities of all N relevant objects (including active satellites) transiting through it. I.e., the criticality of the *j-th* shell is given by the sum of the individual criticalities over all the k objects crossing the shell:

$$\Xi_j = \sum \Xi_{k,j} \tag{10}$$

Finally, the overall criticality for the LEO environment can be estimated as the sum of the Ξ_j over all the M shells in which the LEO region was subdivided.

Recognising the fact that active spacecraft can manoeuvre avoiding collisions, in [20] a more complex formulation of the index was adopted by multiplying the CSI of any object by specific weights accounting for the manoeuvring capabilities, the mitigation/de-orbiting policy, the projected failure rates of each spacecraft, etc. This extended formulation was applied to the evaluation of the environmental criticality of the large LEO constellations. In the present work, we assumed that all the active spacecraft, with linear dimensions larger than 1 m, have collision avoidance capabilities and therefore we multiply the index computed by Eq. (6) by a factor equal to 0.1. That is the weight of that specific spacecraft on the environment is "discounted" by 90% due to its capability of avoiding collisions.

3 CASE SCENARIO AND METHODOLOGY DESCRIPTION

The purpose of this study is to compare the three methods described in the previous section, using a common test case to highlight both their similarities and differences in evaluating space capacity. Specifically, the space consumed capacity is calculated across five altitude bins, focusing on the most relevant shells within LEO (625 km, 775 km, 850 km, 975 km, 1450 km), and considering two bin sizes (10 km and 50 km).

A standardised LEO space object population was used across all three models. It includes all non-decayed, intact (operational payloads, non-operational payloads, and rocket bodies) objects with an apogee less than 2500 km as of January 31, 2025 from the LeoLabs public catalogue. All models incorporated the mass, hard body radius (used to compute the average cross-sectional area), and orbital elements of 12819 objects; the latter includes 979 Rocket Bodies and 11837 Payloads (1757 of which are inactive and 10080 are active). The mass and size of fragments are not considered directly in this catalogue, though their population does introduce collision risk that can be accounted for in modelling.

Each model was used to assess the consumed capacity in the selected bins for the population under analysis, classifying the different shells on a scale from 1 (least consumed) to 5 (most consumed). In addition to assessing ranking differences, the comparison also focused on understanding how normalised capacity (for each model) differs across the three models, in order to determine the relative weight of each bin. The capacity is normalised to standardise the results and place them on a comparable scale. Two types of normalisations are considered: the first is relative to the capacity consumed in the bin with the highest ranking (to show the difference from the other bins), and the second is relative to the total capacity consumed in all five bins (to indicate the share of each bin).

In this way, in addition to identifying which bin is most critical for each model, we can also quantify its relative significance compared to the others. Such information is valuable and necessary for conducting studies on how and when to modify or introduce new guidelines, making certain regions of space more sustainable and less prone to risk. As a result, regulations governing the number of objects orbiting in specific orbital regions can be improved.

4 RESULTS

This section describes the results of each model and their comparison.

Table 1 and Table 2 show the ranking of the orbital shells in the three models for the case with 10 km bin size, respectively considering or excluding operational payloads. Table 3 and Table 4, instead, show the results for the 50 km size case. As a general comment, the altitude bins at 625 km and 1450 km appear to be at lower risk or show lower consumed capacity for all three models. The 850 km shell is identified as the most heavily utilised by all models when using a 50 km bin size. For the THEMIS model, this position is taken by the 775 km bin if operational objects are included, and by the 975 km bin if they are excluded from the analysis, when considering the case of 10 km bin size.

Looking instead at the space capacity normalised relative to the maximum bin, Figure 1 (operational and non-operational) and Figure 2 (non-operational only) show the variation across the bins for the 10 km scenario, while Figure 3 (operational and non-operational) and Figure 4 (non-operational only) display the variation for the 50 km scenario. Table 1

Table 1. Orbit shells ranking according to the consumed capacity level - 10 km bin with operational and non-operational objects.

	625 km	**775 km**	**850 km**	**975 km**	**1450 km**
THEMIS	2	5	4	3	1
CSI	2	3	5	4	1
Risk Balance	1	3	5	4	2

Table 2. Orbit shells ranking according to the consumed capacity level - 10 km bin with non-operational objects.

	625 km	**775 km**	**850 km**	**975 km**	**1450 km**
THEMIS	1	3	4	5	2
CSI	2	3	5	4	1
Risk Balance	1	3	5	4	2

Table 3. Orbit shells ranking according to the consumed capacity level - 50 km bin with operational and non-operational objects

	625 km	**775 km**	**850 km**	**975 km**	**1450 km**
THEMIS	2	4	5	3	1
CSI	2	3	5	4	1
Risk Balance	1	3	5	4	2

Table 4. Orbit shells ranking according to the consumed capacity level - 50 km bin with non-operational objects.

	625 km	**775 km**	**850 km**	**975 km**	**1450 km**
THEMIS	1	3	5	4	2
CSI	2	3	5	4	1
Risk Balance	1	3	5	4	2

Concerning the Risk Balance Model, the manoeuvrability associated with operational payloads is much more comprehensive than the initial model results [cite IAC original paper], though this factor can be further refined to include known operational practices. For this paper, a default manoeuvrability threshold was used for a payload if specific practices were unknown, but the payload was known to be manoeuvrable. The inclusion of operational payloads made the largest impact in the 775 km bin and the 625 km bin. The mass of an object is spread evenly across its entire orbital range in 10 km increments, thus dampening extreme spikes in mass density, which results in the size of the bins (10 km vs 50 km) causing very little change, even in the normalised percentages. If examining impacts across the entirety of LEO, there are orbital shells where operational payloads would have significantly increased consumed capacity, but not the five regions considered in this paper, as the mass of derelicts in these regions far surpassed operational payloads.

It is noted this Risk Balance Model method heavily weights the mass present in an orbital shell over the probability of collision. The large difference in risk normalization seen at 850 km in this model is due to the presence of the large 9,000 kg SL-16 rocket bodies. Other areas with a higher count of objects, but less massive objects are slightly discounted in the current iteration of the Risk Balance Model. A future improvement will be to incorporate the method of 'Probability of Collision by' (PCb) into the algorithm. Doing so will likely de-emphasize the large difference between 850 km and 975 km, as the 975 km altitude bin has a PCb at least four times higher than any other cluster [25]. The PCb is a cumulative Poisson probability for a collision rate between the massive derelicts in each cluster from the time most of the massive objects in these clusters were first abandoned.

Regarding the results using the THEMIS model, some assumptions were made for each object in the list. For each operational payload, two mission phases were considered: the operational phase and the de-orbiting phase. The operational phase, which lasts 8 years for all satellites, provides a 90% effective Collision Avoidance Manoeuvres efficacy. This allows the collision probability calculation to exclude debris that can be tracked from the ground and therefore avoided. The de-orbiting phase, instead, ensures the satellite re-enter within five years, using the King-Hele method [ref]. For non-operational payloads and rocket bodies, only a single phase is considered (i.e., the re-entry phase) assuming natural orbital decay from their initial catalogued positions.

The results indicate that for the 10 km bins, the highest value is found at 775 km, followed by 850 km and 975 km, with the latter two at roughly the same level. When operational objects are excluded, the peak value shifts upwards in these two bins, which again exhibit comparable levels of consumed capacity. This outcome arises from a combination of the collision probability, currently based on the European Space Agency (ESA) MASTER 8 [27] fluxes from the 2016 reference population, and the severity map, which exhibits high values in the Sun Synchronous Orbit (SSO) region. The flux peaks near 800 km, making the 775 km bin particularly significant. Furthermore, excluding active objects reduces the count of objects from an initial 147 (at 775 km) and 144 (at 975 km) to 80 and 141, respectively, thus influencing the final consumed capacity value. By contrast, in the 50 km scenario, this trend is mitigated because more objects (especially inactive ones) fall into each bin, altering the initial distribution.

Similar considerations can be done with the results from the CSI analysis. As in the other cases it has to be noted that in the CSI case the operational objects with dimensions larger than 70 cm are assumed to have a 90 % collision avoidance capability. Smaller spacecrafts are supposed to have not enough manoeuvring capabilities. Given the lower weighting of the operational payloads, no difference is noted between Tables 1 and 2 and between Table 3 and 4. However, assuming no manoeuvring capabilities for all the objects in the sample (case not included in the results from Tab. 1-4), would cause a swap in the ranking between the 775 and 975 km shells, due to the significant change in the number of considered objects, as noted above. As mentioned, the CSI results match closely with the ones of RBM. The main difference being the ranking of the lowest and highest shells, at 625 and 1450 km, respectively. Despite the significant difference in the residual lifetime (fifth term of the CSI in Eq. (6)) in favour of a higher share for the 1450 km shell, its lower ranking is mostly due to the lower median MOID of the objects clustered at that altitude. Finally, it is worth stressing that, despite being identical for the 10 and 50 km shell, a closer analysis of the results of the CSI show a dependence on the shell partitioning of the examined space. In particular, the adopted underlying objects density (fourth term in Eq. (1)) shows significant discontinuities right at the limits of the considered shells. A different partitioning of the altitude shells for the assumed background density might translate in a swapping between the 850 and 975 km shells ranking. This aspect, and its possible implications, will be further investigated in future efforts.

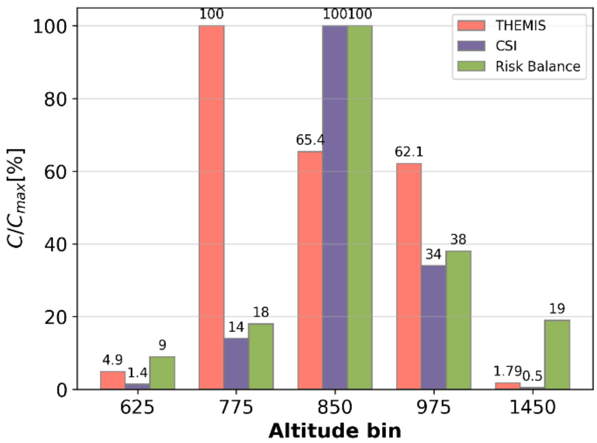

Figure 1.Consumed capacity normalised with respect to the maximum bin value - 10 km bin with operational and non-operational objects.

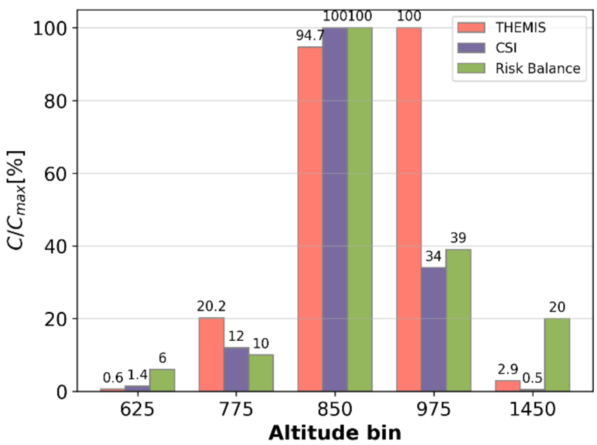

Figure 2. Consumed capacity normalised with respect to the maximum bin value - 10 km bin with non-operational objects.

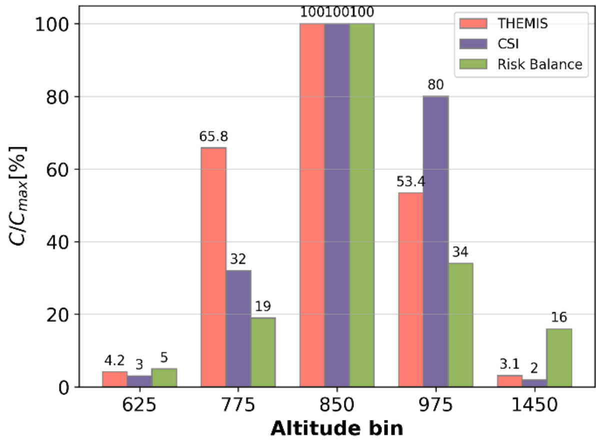

Figure 3. Consumed capacity normalised with respect to the maximum bin value - 50 km bin with operational and non-operational objects.

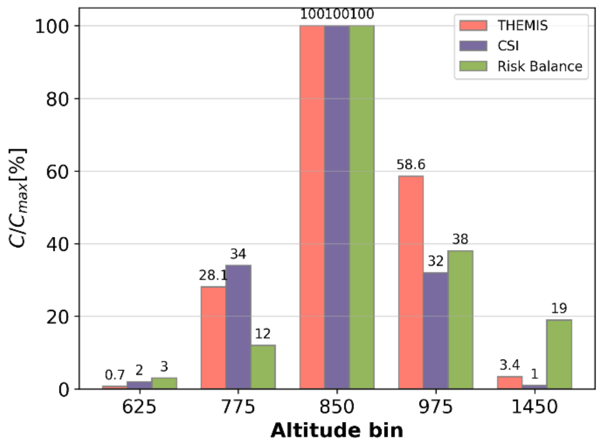

Figure 4. Consumed capacity normalised with respect to the maximum bin value - 50 km bin with non-operational objects.

A different perspective involves examining the fraction of capacity consumed in each bin, computed as the ratio of that bin to the total capacity consumed across all bins, for the three models; Figure 5, Figure 6, Figure 7, and Figure 8 present the results for the four scenarios.

An important observation is that, within the RBM framework, the 850 km bin consistently exceeds 50%, indicating a dominant contribution relative to the other bins. For the same bin in the CSI model, the share is above 50% when the bin size is 10 km, but drops below 50% when the bin size is 50 km. In contrast, under THEMIS, the share remains below 50% except when the bin size is 50 km and only non-operational objects are considered.

Focusing on the 775 km bin, in both the CSI and RBM models its share remains below 20%. The same is valid for the THEMIS model when operational objects are excluded; once those are included, the share rises above 20% and can even exceed 40% in the 10 km bin scenario.

For the RBM, the 975 km bin has a share of around 20%, while both THEMIS and CSI estimate its share between 20% and 45%.

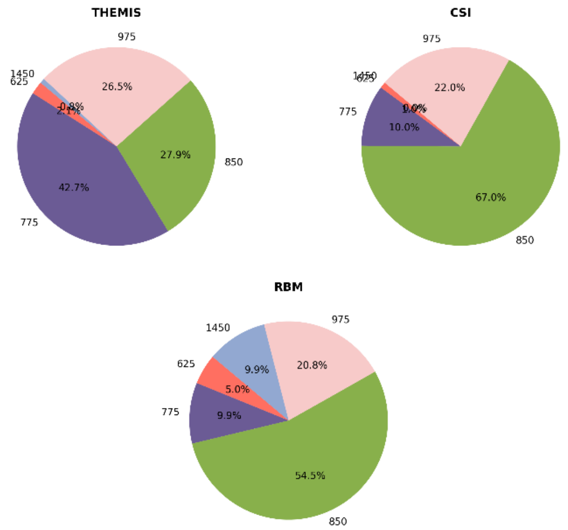

Figure 5. Share of consumed capacity in each bin - 10 km bin with operational and non-operational objects.

Figure 6. Share of consumed capacity in each bin - 10 km bin with non-operational objects.

These results indicate that the RBM model's capacity estimates are relatively insensitive to the inclusion of operational satellites in the population (and only slightly affected by bin size). In contrast, the THEMIS model exhibits sensitivity to both the presence of active objects and the chosen bin dimension. The CSI model shows a dependence on bin size, similar to THEMIS.

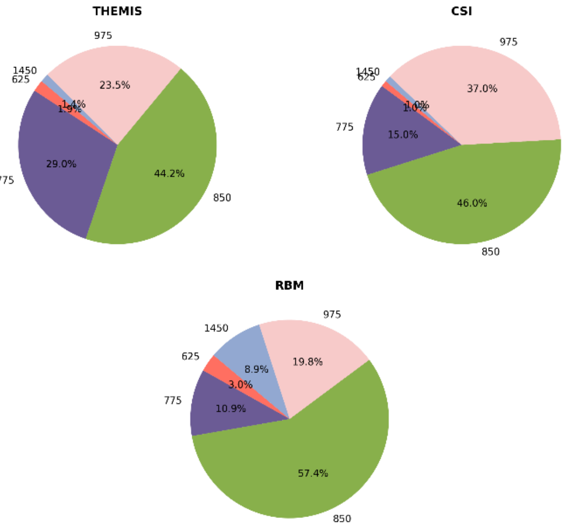

Figure 7. Share of consumed capacity in each bin - 50 km bin with operational and non-operational objects.

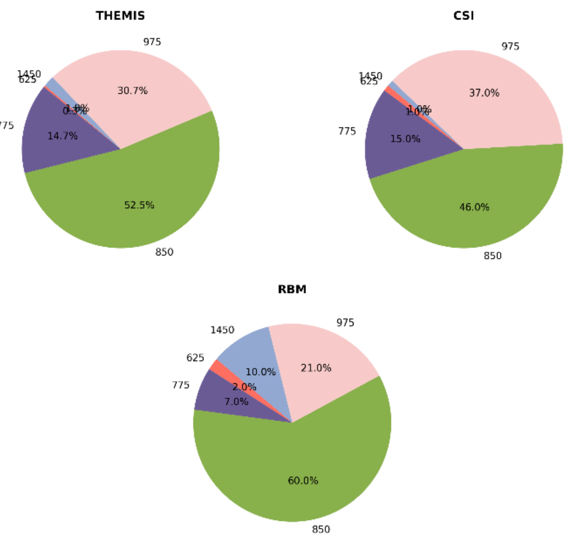

Figure 8. Share of consumed capacity in each bin - 50 km bin with non-operational objects.

5 CONCLUSION

The objective of this work was to compare three models for evaluating space capacity, using the same scenario in all three cases while considering possible variations introduced by specific parameters. In particular, the study focused on how different bin sizes affect capacity assessments and on the changes in the assessment when operational satellites are either included or excluded from the analysis.

In all cases, the three models agree in distinguishing between the two lower-risk regions (625 km and 1450 km) and the higher-risk regions (775, 850, and 975 km). Overall, they generally identify 850 km as carrying the highest risk.

Some discrepancies were observed in the THEMIS model, which does not assign the highest rank to the 850 km bin when using a 10 km bin size. This discrepancy may stem from the model's method of weighting operational and non-operational objects, leading to a different assessment of each mission's impact relative to the other models. Additional analyses will be carried out in future work.

In general, the three models exhibited overall alignment, yet further analysis of the variation in the normalised index is needed. This will be addressed in future works, where additional parameters, such as inclination and object mass, will be also investigated.

Acknowledgments

The work of A.M., C.C and A.R. was performed under financing from the Italian Space Agency (ASI Contract "Detriti Spaziali - Supporto alle attività IADC e SST 2023-2025").

References

1. ESA Space Debris Office (2024), ESA's Annual Space Environment Report. Technical Report.

2. Anz-Meador, P., Opiela, J., and Liou, J.-C. (2022). History of On-orbit Satellite Fragmentations, 16th Edition. Technical Report NASA/TP-20220019160

3. McKnight D., Witner R., Letizia F., Lemmens S., Anselmo L., Pardini C., Rossi, A., Kunstadter C., Kawamoto S., Aslanov V., Dolado Perez J.-C., Ruch V., Lewis H., Nicolls M., Jing L., Dan S., Dongfang W., Baranov A., Grishko D. (2021). Identifying the 50 statistically-most-concerning derelict objects in LEO. *Acta Astronautica,* pp.282-291. Doi: https://doi.org/10.1016/j.actaastro.2021.01.021

4. Letizia F., Colombo C., Rossi A., Muciaccia A., Giudici L., Harada R., Kawamoto S., Böttcher L., Ruch V., Taillan C. (2024). Mission-based and environment-based approaches for assessing the severity of a space debris evolution scenario from a sustainability perspective. In proceedings of: 75th International Astronautical Congress (IAC), Milan, Italy.

5. Liou J.-C.& Johnson N. L. (2009). A sensitivity study of the effectiveness of active debris removal in LEO. *Acta Astronautica*. pp. 236-243. Doi: https://doi.org/10.1016/j.actaastro.2008.07.009

6. Rossi A., G.B. Valsecchi, E.M. Alessi, (2015). The Criticality of Space Index, *ASR,* Vol 56, Issue 3, ppg. 449-460. Doi: https://doi.org/10.1016/j.asr.2015.02.027

7. Letizia F., Colombo C., Lewis H. G., & Krag H. (2016). Assessment of breakup severity on operational satellites. *Advances in Space Research* pp. 1255–1274. doi: https://doi.org/10.1016/j.asr.2016.05.036

8. Pardini C. and Anselmo L. (2018). Evaluating the environmental criticality of massive objects in LEO for debris mitigation and remediation. *Acta Astronautica*. pp. 51–75 doi: https://doi.org/10.1016/j.actaastro.2018.01.028

9. Colombo C., Muciaccia, A., Giudici, L., Gonzalo, J.L., Masat, A., Trisolini, M., Del Campo, B., Letizia, F., Lemmens, S. (2023). Tracking the Health of the Space Debris Environment with THEMIS. Aerospace Europe Conference 2023 - Joint 10th EUCASS - 9th CEAS Conference

10. Harada R., Kawamoto S., & Hanada T. (2024). Establishment of debris index evaluation criteria and comparison of index effects. *Acta Astronautica*. pp. 586–595. Doi: https://doi.org/10.1016/j.actaastro.2024.06.047

11. Kessler D. J. & Anz-Meador P. D. (2001). Critical Number of Spacecraft in Low Earth Orbit: Using Satellite Fragmentation Data to Evaluate the Stability

of the Orbital Debris Environment. In Proceedings of 3rd European Conference on Space Debris, Germany, European Space Agency (ESA)

12. Bötcher B. & Silvestri S. (2024). In-depth characterisation of a criticality metric. In Proceedings of the 45th COSPAR, Bexco, Busan, South Korea.

13. Bologna D. G., Henning G. A., Sorge M. E., Peterson G. E., Mains D. L., & Maldonado J. C. (2023). Conjunction Frequency-Based Sustainability Assessment of Future LEO Activity. In Proceedings of the 2nd Orbital Debris Conference.

14. Wang Y., Wilson C., & Vasile M. (2023). Multi-Layer Temporal Network Model of the Space Environment. In Proceedings of AAS Conference

15. D'Ambrosio A. & Linares R. (2024). Carrying Capacity of Low Earth Orbit Computed Using Source-Sink Models. *Journal of Spacecraft and Rockets*. pp. 1447-1463, Doi: https://doi.org/10.2514/1.A35729

16. Muciaccia, A., Letizia F., Trisolini M., Giudici L., Lemmens S., Gonzalo J. L., Colombo, C, (2024). Low Earth Orbit capacity thresholds investigation for a sustainable use of the space environment, 75th International Astronautical Congress (IAC)

17. Colombo C., Giudici L., Muciaccia A., Gonzalo J. L., Borja D. C., Vyavahare N., Dutra D., Letizia F., & Lemmens S. (2023). Assessment of the collision risk in orbital slots and the overall space capacity. In Proceedings of 2nd International Orbital Debris Conference, Sugar Land, Texas.

18. Muciaccia A., Trisolini M., Giudici L., Gonzalo J. L., Colombo C., & Letizia F. (2023). Influence of Constellations on Current and Future Missions. 2nd International Orbital Debris Conference, Sugar Land, Texas.

19. Bombardelli C., E.M. Alessi, A. Rossi, G.B. Valsecchi., (2017). Environmental effect of space debris repositioning, *ASR*, Vol 60, Issue 1, ppg.28-37.

20. Rossi A., E.M. Alessi, G.B. Valsecchi, H. Lewis, J. Radtke, C. Bombardelli, B. Bastida Virgili, (2017). A quantitative evaluation of the environmental impact of the mega constellations, Proc. 7th European Conference on Space Debris, 18–21 April 2017, Darmstadt, Germany.

21. Rossi A., L. Anselmo, C. Pardini, R. Jehn, G. B. Valsecchi, (2009). The new space debris mitigation (SDM 4.0) long term evolution code, in 5th European Conference on Space Debris, ESA Special Publication, Vol. vol. 672, p. 90.

22. G.F. Gronchi, (2002). On the stationary points of the squared distance between two ellipses with a common focus, SIAM J. Sci. Comput. 24/1, 61–80.

23. G.F. Gronchi, (2005). An algebraic method to compute the critical points of the distance function between two Keplerian orbits, Celestial Mech. Dyn. Astron., 93/1, 297–332.

24. Rossi A., A. Petit. D. McKnight, (2020). Short-term space safety analysis of LEO constellations and clusters, *Acta Astronautica*, 175, 476–483

25. McKnight, D., Dale, E., Kunstadter, C. (2024). Modelling Short-term Space Object Population Growth in LEO. In Proceedings of International Astronautical Congress, Milan, Italy.

26. King-Hele, D. (1964). Theory of Satellite Orbits In an Atmosphere. *Quarterly Journal of the Royal Meteorological Society*. pp. 503-504. Doi: https://doi.org/10.1002/qj.49709038627

27. Horstmann A., Hesselbach S., Wiedemann C., Flegel S., Oswald M., & Krag H. (2020). Enhancement of S/C Fragmentation and Environment Evolution Models, ESA Contract No. Tech. rep. 4000115973/15/D/SR.